Journal of Solid State Chemistry 182 (2009) 3289–3293

Contents lists available at ScienceDirect

Journal of Solid State Chemistry

journal homepage: www.elsevier.com/locate/jssc

Theoretical investigation of structural stability and lattice vibrations of $U_6Fe_{16}Si_7$ and its interstitial carbide $U_6Fe_{16}Si_7C$

Ping Qian [a,*], Qing-Yu Hu [b], Jiang Shen [a]

[a] Institute of Applied Physics, Beijing University of Science and Technology, Beijing 100083, China
[b] Dancheng Bureau of Education, Dancheng 477150, China

ARTICLE INFO

Article history:
Received 28 July 2009
Received in revised form
11 September 2009
Accepted 20 September 2009
Available online 30 September 2009

PACS:
81.05.Zx
34.20.Cf
63.20.Dj

Keywords:
Interatomic potentials
Crystal structure
Actinide compounds
Lattice dynamics

ABSTRACT

A series of lattice inversion pair potentials are used to evaluate the phase stability and site preference for uranium intermetallics $U_6Fe_{16}Si_7$ and its interstitial carbide $U_6Fe_{16}Si_7C$. The calculated preferentially occupation site of the Si atom is found to be the 4*a* site. Interstitial C atom can only be located on the 4*b* site. Calculated lattice constants are found to agree with a report in the literature. It is noted that the total and partial phonon densities of states are first evaluated for the $U_6Fe_{16}Si_7$ and $U_6Fe_{16}Si_7C$ compounds. The analysis for the inverted potentials explains qualitatively the contributions of different atoms to the vibrational modes.

1. Introduction

New ternary intermetallic compounds containing uranium, a transition metal and an element of the *p*-block have attracted widespread attention for the study of fundamental aspects of magnetism [1–5]. Examples of complex magnetic behaviors and rich magnetic phase diagrams are legion. It is commonly assumed that the variety of magnetic phenomena of the U-based compounds is due to the specific nature of the 5*f* electrons, which cover a wide range between localized and itinerant behaviors. The degree of delocalization (or localization), which occurs either via the direct overlap of the 5*f*-electron shells of the neighboring U atoms, or the 5*f*-ligand hybridization, governs the magnetic properties. In recent years, Chen et al. have performed a theoretical study on the structural properties for the rare-earth compounds with 4*f* electron and actinide compounds with 5*f* electron [6–15]. The method combining interatomic potentials with different crystal structures is a shortcut but effective way to investigate the structural stability and the site preference. It is accepted that the local atomic environment determines if the energy of a compound is low enough to form a compound with a certain structure. In this work, the interatomic potentials acquired by Chen's lattice inversion method are used to investigate the lattice constants and site preference of the new uranium and iron intermetallics, $U_6Fe_{16}Si_7$ and $U_6Fe_{16}Si_7C$. In addition, the phonon density of states (DOS) of these uranium intermetallics is evaluated, from which the Debye temperatures are obtained.

2. Computational method

The atomistic simulation has been widely used in the investigation of the properties and behaviors of various materials. One of the key problems in atomistic simulation method is the determination of the interatomic potentials. On the basis of Möbius inversion in the number theory, Chen et al. proposed a concise inversion theorem to obtain intermetallic pair potentials from the cohesive energy curves [16,17]. And it has been applied successfully to study the phase stability, the site preference of ternary additions, the lattice dynamics, and so on. In our previous works [11,13–15], the methods of obtaining the potentials have been reported in detail. The inverted pair potentials from the cohesive energy are approximately expressed as Morse function

$$\Phi(x) = D_0(e^{[-\gamma(x/R_0-1)]} - 2e^{[-(\gamma/2)(x/R_0-1)]}) \quad (1)$$

where D_0, R_0, γ are potential's parameters. For the reader's convenience, several important potential parameters are listed in Table 1.

* Corresponding author. Fax: +86 10 62322872.
E-mail address: qianpinghu@sohu.com (P. Qian).

0022-4596/$ - see front matter © 2009 Elsevier Inc. All rights reserved.
doi:10.1016/j.jssc.2009.09.023

3. Phase stability and site preference

Experiments [18] have pointed out that $U_6Fe_{16}Si_7$ and $U_6Fe_{16}Si_7C$ crystallize with the ternary ordered variant of the Th_6Mn_{23}-type, commonly referred as $Mg_6Cu_{16}Si_7$ and with a novel "filled" variant of this type of structure, respectively. In order to study the effect of Si atoms on the structure stability of $U_6Fe_{16}Si_7$ compounds, we investigated theoretically the substitution behaviors of Si in $U_6Fe_{23-x}Si_x$ compounds with the Th_6Mn_{23}-type structure. In a typical crystal cell with four $U_6Fe_{23-x}Si_x$ molecular formulas (116 atoms per unit cell), there are four nonequivalent sites $32f_1$, $32f_2$, 24*d*, 4*b* for Fe or Si and one site 24*e* for Th atoms. In the simulation process, firstly the virtual binary U_6Fe_{23} structure can be considered as intrinsic structure of $U_6Fe_{23-x}Si_x$ compounds. And based on the atomic sites and lattice parameters of any existing experimental [19–21] structure close to Th_6Mn_{23}-type with the $Fm\bar{3}m$ (No. 225) cubic space group, initial U_6Fe_{23} is constructed within Accelrys Cerius 2 modeling software. Then we introduced relaxation governed by the energy minimization process, using conjugate gradient method with a cut-off radius of 14 Å. Once the energy minimization process based on inverted pair potential carried out, the initial structure will reach a stabilized structure with minimized cohesive energy, provided that the initial model can be identified as the existing Th_6Mn_{23}-type structure with $Fm\bar{3}m$ space group. The atomic sites of the final U_6Fe_{23} structure are evaluated and listed in Table 2.

Table 1
Part of Morse parameters of the conversed pair potentials.

	R_0 (Å)	D_0 (eV)	γ
U–U	3.9415	0.6624	7.3445
Fe–Fe	2.7361	0.7640	8.7529
C–C	2.8178	0.3854	7.1673
Si–Si	3.4427	0.3835	7.3164
U–Fe	3.2024	0.8835	8.6841
U–Si	3.4088	0.7352	8.4856
U–C	3.0005	0.9739	8.1970
Fe–Si	2.7334	0.6632	8.2601
Fe–C	2.4901	0.7214	7.9375
C–Si	3.0976	0.3934	6.5905

Table 2
Atomic parameters of U_6Fe_{23}.

Atom	Wyckoff position	*x*	*y*	*z*
U	24*e*	0.2806	0	0
Fe(1)	$32f_1$	0.1181	0.1181	0.1181
Fe(2)	$32f_2$	0.3257	0.3257	0.3257
Si(1)	24*d*	0	1/4	1/4
Si(2)	4*b*	1/2	1/2	1/2

Based on the binary compounds U_6Fe_{23}, the dependences of the cohesive energy and tolerance of $U_6Fe_{23-x}Si_x$ on the content of ternary addition are evaluated. In order to reduce statistical fluctuation, we adopt the model of $3\times3\times3$ periodical super-cell, containing 3132 atoms. The calculated cohesive energy and tolerance of $U_6Fe_{23-x}Si_x$ are shown in Fig. 1 when Si atoms occupy the $32f_1$, $32f_2$, 24*d* and 4*b* sites, respectively. The tolerance, which represents the atomic derivation distance can be viewed as the errors in the process of determining the space group of the compound, is an assistant criterion. Numerous calculations show that, when the tolerance is much larger than 0.6 Å, the structure does not exist in experiments. It is found in Fig. 1 that the cohesive energies of $U_6Fe_{23-x}Si_x$ except for $x=1.00$ are similar when Si atoms occupy different sites. But the tolerance is so large that the $U_6Fe_{23-x}Si_x$ compounds with the structure of Th_6Mn_{23} could not be stable. When $x=1.00$, the energy of the 4*b* sites rapidly rises and the tolerance suddenly drops down to 0.01 Å. This is because the Si atoms at the particular sites are all substituted, and the structure of the system is very symmetric.

The newest experiment [18] shows that Si atoms are seated in 24*d* and 4*a* sites in $U_6Fe_{16}Si_7$ compound. To check this, we calculate the cohesive energies and tolerances of Si atoms substituting for Fe at each site including $32f_1$, $32f_2$, 24*d* and 4*a* sites. The calculated results are plotted in Fig. 2. The figure clearly shows that within $x<1.00$ the cohesive energy is lower when Si atoms are substituted for Fe at the 4*a* sites than for ones at the 24*d*, $32f_1$ and $32f_2$ sites, and the tolerance is acceptable. So, in the calculation, Si atom preferentially occupies the 4*a* site based on the cohesive energy and tolerance considerations when $x<1.00$. Within the composition range $x>1.00$, four Si atoms have already occupied the 4*a* sites based on the above analysis, so the remaining Si atoms can only occupy the 24*d*, $32f_1$ or $32f_2$ sites. The cohesive energies and tolerances are lowest when Si atoms are at 24*d* sites. So when $x>1.00$, Si atoms prefer the 24*d* sites besides four Si atoms occupying the 4*a* sites. The first silicon atoms to enter the structure fill a high percentage of the 4*a* sites, after which, occupation of the 24*d* sites begin, which is consistent with the $Mg_6Cu_{16}Si_7$-type structure in the experiment [18]. The calculated results also show that the cohesive energy of $U_6Fe_{23-x}Si_x$ increases with the increase of Si content, which indicates that the addition of Si decreases the stability of U–Fe–Si systems.

Further, the relationship of the cohesive energy of $U_6Fe_{16}Si_7C_x$ and the content of interstitial C atoms are investigated, where seven Si atoms occupy the 24*d*, 4*a* sites and the C atoms the 4*b* sites randomly. The calculated average energies of $U_6Fe_{16}Si_7C_x$ are −7.2709, −7.2599, −7.2477, −7.2332 and −7.2166 eV/atom for

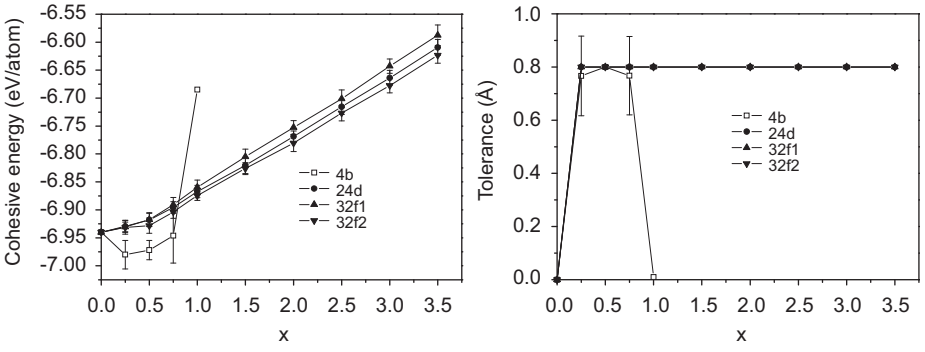

Fig. 1. Energy and tolerance variation in $U_6Fe_{23-x}Si_x$ with Si occupying different $32f_1$, $32f_2$, 24*d* and 4*b* sites, respectively.

x=0.00, 0.25, 0.50, 0.75 and 1.00, respectively. The structure calculations of $U_6Fe_{16}Si_7C_x$ retain $Fm\bar{3}m$ symmetry within a tolerance range of 0.01–0.10 Å. The case of C atoms occupying other interstitial sites is unstable, and the carbon cannot retain its original structure. It means that C atoms only occupy interstitial 4*b* sites in the interstitial carbide $U_6Fe_{16}Si_7C_x$, which is very much consistent with the experimental results [18].

According to the results for the site preference, the lattice constants and the atomic positions of $U_6Fe_{16}Si_7$ and $U_6Fe_{16}Si_7C$ are calculated when Si atoms are in 24*d*, 4*a* sites and C atoms in interstitial 4*b* sites. Calculated lattice constants and atomic positions of $U_6Fe_{16}Si_7$ and $U_6Fe_{16}Si_7C$ are listed in Table 3 together with the experimental data from the literature [18]. Table 3 shows that our results agree with the experimental data.

The stability of $U_6Fe_{16}Si_7$ and its interstitial carbide is investigated by a high temperature disturbance using molecular dynamics. The simulation temperature range is 100–700 K with a step of 200 K. For each temperature and at 1 atm pressure calculations are performed for 40 000 steps with a time step of 2.0×10^{-15} s. During the simulation, the constant-NPT ensemble [22] is used, and the extended system with thermostat and barostat relaxation time of 0.10 ps is adopted. After reaching equilibrium, the crystal symmetry retain the initial $Fm\bar{3}m$ cubic space group within a certain tolerance range at finite temperatures of 100–700 K. Lattice constants are found to change very little with respect to the temperature variation and the phase stability is thus verified.

4. Lattice dynamic simulations

Phonon density of states (DOS) reflects the lattice dynamic properties, from which some important thermodynamic parameters can be derived. In this subsection, with the inverted interatomic potentials, the total DOS as well as the partial DOS of $U_6Fe_{16}Si_7$ and its interstitial carbide $U_6Fe_{16}Si_7C$ intermetallics are firstly studied at an atomistic level. The calculated result (Fig. 3) exhibits the contributions to DOS of distinct atoms. It is seen that the highest frequency of $U_6Fe_{16}Si_7$ is 9.77 THz, and two localized mode whose frequencies are higher than 7.56 THz. From the partial DOS it may be inferred that the vibrational modes are mostly excited by Fe atoms in the range of 3.31–7.06 THz. U largely contributes to modes with lower frequencies. The high frequency localized modes are almost excited by Si atoms. In the $U_6Fe_{16}Si_7C$ compound, the phonon densities of states are similar with that of $U_6Fe_{16}Si_7$. C, however, only contributes to modes at 11.99 THz.

One can analyze qualitatively the vibrational modes from interaction potentials (Fig. 4) and the nearest neighbor distances between the atoms. For $U_6Fe_{16}Si_7$ four Fe atoms are present at the $32f_1$ site, four Fe atoms are at the $32f_2$ sites and four Si atoms are

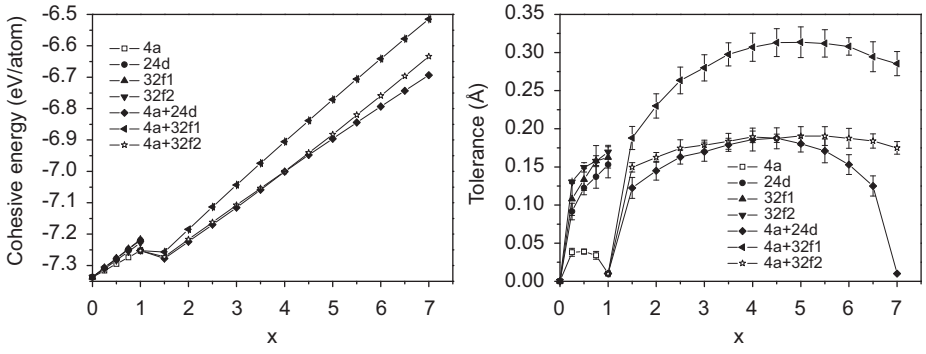

Fig. 2. Energy and tolerance variation in $U_6Fe_{23-x}Si_x$ with Si occupying different $32f_1$, $32f_2$, 24*d* and 4*a* sites, respectively.

Table 3
Lattice parameter *a* and atomic positions of $U_6Fe_{16}Si_7$ and $U_6Fe_{16}Si_7C$ with the experimental data [18] in brackets.

Compounds	*a* (Å)	U, 24*e*, *x*	Fe(1), $32f_1$, *x*	Fe(2), $32f_2$, *x*	Si(1), 24*d*, *y*	Si(2), 4*a*, *z*	C, 4*b*, *z*
$U_6Fe_{16}Si_7$	11.9693 (11.7206)	0.2999 (0.2859)	0.1186 (0.1212)	0.3249 (0.3276)	1/4 (1/4)	0 (0)	
$U_6Fe_{16}Si_7C$	12.1081 (11.7786)	0.2866 (0.2894)	0.1206 (0.1222)	0.3254 (0.3255)	1/4 (1/4)	0 (0)	1/2 (1/2)

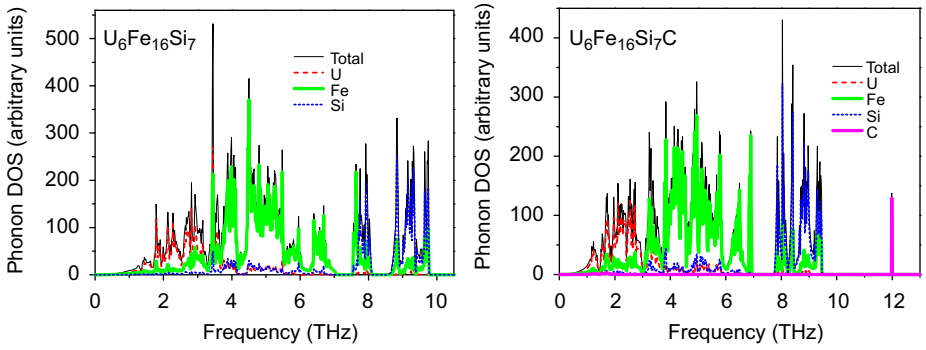

Fig. 3. Phonon densities of states of $U_6Fe_{16}Si_7$ and $U_6Fe_{16}Si_7C$.

at the 24*d* sites around U. Distances between U–Fe ($32f_1$), U–Fe ($32f_2$) and U–Si (24*d*) are 2.856, 2.981 and 3.051 Å, respectively. As shown in Fig. 4, the potentials change steeply at these distances which means U reacts strongly with Fe and Si at these distances. The mass of U is much larger than that of Si and is thus assumed motionless relative to the Si atom. Some Si atoms are restricted to the 'potential well' $\Phi_{U-Si}(r)$. This might be the reason for the appearance of Si-localized modes that correspond to the higher transected frequency. U atoms only contribute to lower frequency vibrations in the U–Si 'potential well' because of their large atomic mass. Furthermore, the nearest distance between Fe and Si is 2.450 Å and Fe thus reacts strongly with these Si atoms. This means that the Si atoms contribute to higher frequency modes because of the light Si. The mass of Fe is approximately twice larger than that of Si, so Fe atoms can be strongly excited by more modes with lower frequency than the Si atoms due to the heavy mass of Fe. Comparing with the contribution of U atom to the low frequency modes, as Fe atom is lighter than U atom, the Fe atom mostly contributes to the spectra in the range of 3.31–7.06 THz. For $U_6Fe_{16}Si_7C$ the optic modes are far separated from the acoustic modes and have very high frequencies which are due to the large mass difference in the atoms and the strong force constants between nearest neighbors U and carbon atoms.

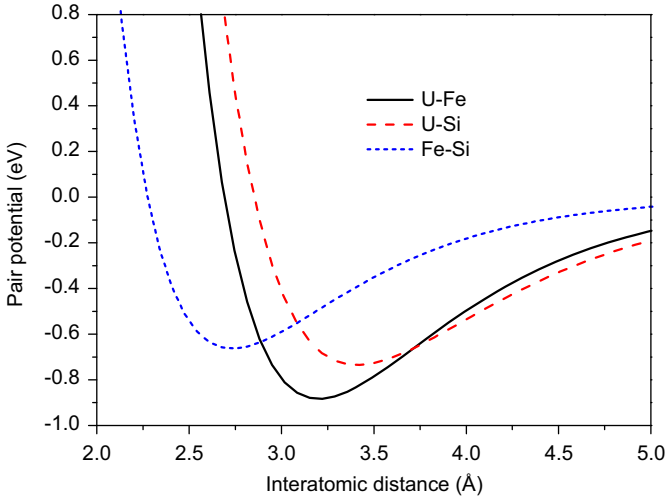

Fig. 4. Potentials of U–Fe, U–Si and Fe–Si.

Furthermore, the specific heat, vibrational entropy and Debye temperature can be obtained by the calculated phonon DOS. Fig. 5 gives the calculated lattice specific heat, vibrational entropy and Debye temperature of $U_6Fe_{16}Si_7$ and $U_6Fe_{16}Si_7C$ as a function of temperature. The figure clearly shows that the values of the specific heat and vibrational entropy are larger for $U_6Fe_{16}Si_7C$ than that for $U_6Fe_{16}Si_7$. The Debye temperature reflects the property of the materials at the lower temperature and lower frequency. For $T \approx 0$ K, the Debye temperatures of $U_6Fe_{16}Si_7$ and $U_6Fe_{16}Si_7C$ are 340 and 315 K, respectively. Apparently, the Debye temperature decreases when interstitial C atoms are introduced into the $U_6Fe_{16}Si_7$ compound. Therefore, C may play an important role in the lower-temperature properties of these materials.

5. Conclusion

In the present paper, structural properties of $U_6Fe_{16}Si_7$ and its interstitial carbide $U_6Fe_{16}Si_7C$ are investigated by using the interatomic pair potentials obtained with the lattice inversion method. Calculated results demonstrate that Si atoms preferentially occupy 4*a* sites. Interstitial C atoms only occupy 4*b* interstitial sites in $U_6Fe_{16}Si_7C$. The calculated results reported correspond well to the available experimental data. Again, we utilize these potentials to evaluate the thermodynamic properties of these actinide compounds.

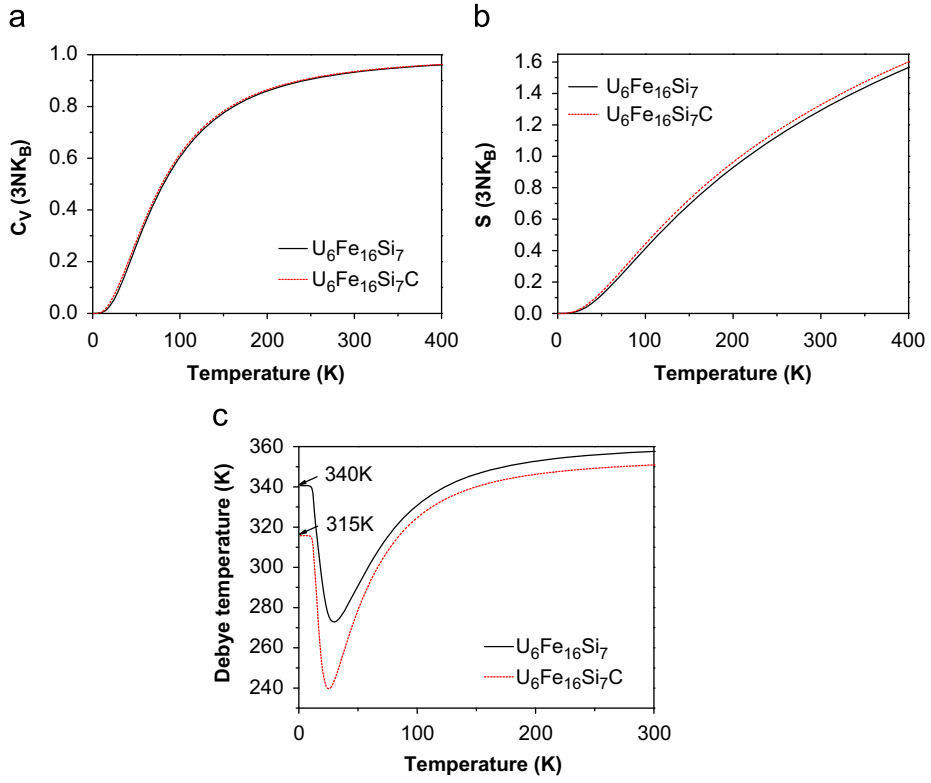

Fig. 5. Calculated specific heat, vibrational entropy and Debye temperature of $U_6Fe_{16}Si_7$ and $U_6Fe_{16}Si_7C$.

Acknowledgments

The authors would like to thank Professors F.M. Yang and J.K. Liang at Institute of Physics in the Chinese Academy of Sciences for interesting discussions and encouragement. The work was supported by the 973 Project in China (no. 2006CB605101) and the National Nature Science Foundation of China (Grant no. 50971024).

References

[1] C. Geibel, A. Böhn, R. Caspary, K. Gloos, A. Grauel, P. Hellmann, R. Modler, C. Schank, G. Weber, F. Steglich, Physica B 186–188 (1993) 188–194.
[2] G. André, F. Bourée, A. Oleoe, W. Sikora, B. Pene, A. Szytula, Z. Tomkowicz, Solid State Commun. 97 (1996) 923–929.
[3] S. Pechev, T. Roisnel, B. Chevalier, B. Darriet, J. Etourneau, Solid. State. Sci. 2 (2000) 773–780.
[4] O. Tougait, H. Noël, R. Troc, Solid State Chem. 177 (2004) 2053–2057.
[5] H. Noël, O. Tougait, R. Troc, V. Zaremba, Solid. State. Sci. 7 (2005) 780–783.
[6] H. Chang, N.X. Chen, J.K. Liang, G.H. Rao, J. Phys: Condens. Matter. 14 (2002) 1.
[7] S.Q. Hao, N.X. Chen, J. Shen, J. Alloys. Compd. 343 (2002) 53–59.
[8] W.X. Li, L.Z. Cao, J. Shen, N.X. Chen, B.D. Liu, J.L. Wang, G.H. Wu, F.M. Yang, Y.X. Li, J. Appl. Phys. 93 (2003) 6921.
[9] N.X. Chen, J. Shen, X.L. Wang, J. Alloy Compd. 359 (2003) 91–98.
[10] Y.M. Kang, N.X. Chen, J. Shen, J. Magn. Magn. Mater. 256 (2003) 381–389.
[11] P. Qian, Q.L. Wang, N.X. Chen, J. Shen, J. Phys. D: Appl. Phys. 39 (2006) 1197–1203.
[12] P. Qian, H.J. Tian, J. Shen, N.X. Chen, J. Solid State Chem. 181 (2008) 983.
[13] H.J. Tian, P. Qian, J. Shen, N.X. Chen, Comput. Mater. Sci. 44 (2008) 702–706.
[14] P. Qian, N.X. Chen, J. Shen, Physics Letter. Lett. A 335 (2005) 464–470.
[15] J. Shen, P. Qian, N.X. Chen, Modelling. Simul. Mater. Sci. Eng. 13 (2005) 239–247.
[16] N.X. Chen, G.B. Ren, Phys. Rev. B 45 (1992) 8177.
[17] N.X. Chen, Z.D. Chen, Y.C. Wei, Phys. Rev. E 55 (1997) R5.
[18] D. Berthebaud, O. Tougait, M. Potel, E.B. Lopes, A.P. Goncalves, H. Noël, J. Solid State Chem. 180 (2007) 2926–2932.
[19] J. Ostoréro, J. Alloy Compd. 317–318 (2001) 450–454.
[20] J. Ostoréro, V. Paul-Boncour, F. Bourée, G. André, J. Alloy Compd. 404–406 (2005) 191–194.
[21] X.A. Chen, W. Jeitschko, M.H. Gerdes, J. Alloy Compd. 234 (1996) 12–18.
[22] S. Melchionna, G. Ciccotti, B.L. Holian, Mol. Phys. 78 (1993) 533.